CHALMERS
UNIVERSITY OF TECHNOLOGY

PHASE TRANSFORMATION MECHANISMS IN BORON ALLOYED TI-6AL-4V WELD STUDIED USING BETA GRAIN

Downloaded from: https://research.chalmers.se, 2026-10-08 04:00 UTC

Citation for the original published paper (version of record):
Tolvanen, S., Pederson, R., Klement, U. (2023). PHASE TRANSFORMATION MECHANISMS IN BORON ALLOYED TI-6AL-4V WELD STUDIED USING BETA GRAIN RECONSTRUCTION. Proceedings of the 15th World Titanium Conference Ti 2023(14): 24-29

N.B. When citing this work, cite the original published paper.

research.chalmers.se offers the possibility of retrieving research publications produced at Chalmers University of Technology. It covers all kind of research output: articles, dissertations, conference papers, reports etc. since 2004. research.chalmers.se is administrated and maintained by Chalmers Library

(article starts on next page)

PHASE TRANSFORMATION MECHANISMS IN BORON ALLOYED TI-6AL-4V WELD STUDIED USING BETA GRAIN RECONSTRUCTION

Sakari Tolvanen[1], Robert Pederson[2], Uta Klement[1]

1 Department of Industrial and Materials Science, Chalmers University of Technology, S-412 96 Gothenburg, Sweden
2 Department of Engineering Science, University West, SE-461 86 Trollhättan, Sweden

Substantial effort is put on decreasing the size of both β grains and α colonies of cast, additively manufactured and welded titanium alloys. To evaluate the effect of these efforts, effective methods to characterize the size and orientation of β grains over relatively large regions are needed. In the present work the microstructure of a laser weld in cast Ti-6Al-4V alloy with 0.11 wt.% boron has been studied. Electron back scatter diffraction technique was used to capture a low magnification orientation map of the alpha phase across different weld zones. A method of prior β grain reconstruction based on Burgers orientation relationship was applied to study the prior β grain structure in the different weld zones. The prior β grain reconstruction could be performed successfully and the reliability of the reconstruction was evaluated. The fine microstructure in the weld zones together with low magnification resulted in a relatively low indexing rate in the fusion zone and heat affected zone but this did not affect the quality of prior β grain reconstruction. Analysis of the variant selection and orientation deviation in the reconstructed β grains can give information about the transformation mechanisms in the different weld zones.

Keywords: Grain refinement, boron, EBSD, phase transformation

1. Introduction

Titanium alloys are widely used in medical and aerospace industry. In fabrication of light weight aerospace structures, welding and additive manufacturing are key processes. The microstructure of welded and additively manufactured α-β titanium alloys are typically characterized by coarse prior β grains, occasionally with a continuous α layer at the prior β grain boundaries and acicular microstructure consisting of fine α' and/or α plates separated by thin layers of β phase [1], [2]. On one hand, the fine acicular microstructure contributes to the high strength of additively manufactured and welded titanium alloys but on the other hand, these factors also lower the ductility of Ti-6Al-4V welds [3,4]. Much effort has been put on decreasing the size of both β grains and α colonies. Boron addition has been found to induce significant grain refinement in castings [6]–[8], welds and additively manufactured components [9]–[11]. High cooling rates in welding and additive manufacturing also renders a fine microstructure which makes resolving α colonies and prior β grains difficult using optical microscopy [9].

Effective methods are needed to characterize the size and orientation of β grains over relatively large regions to evaluate grain refinement, in order to optimize the processing parameters, heat treatments as well as the chemistry of the alloys. The use of electron backscattered diffraction (EBSD) technique allows measurement of α phase orientations and colony size distributions in titanium alloys [12], [13]. Because the α and β phases are strictly related by the Burgers orientation relationship, it is possible to deduce the high temperature β phase grains and their orientation from measured α phase orientations [14]. Methods for prior β grain reconstruction have been developed by several researchers [13], [15]–[17]. They have the advantage of also providing the crystallographic orientations of the parent grains which allows the study of variant selection and transformation mechanisms.

In the present work, EBSD analysis combined with the *Merengue 2* software, developed by Germain et al. [17], have been used to perform prior β grains reconstruction in a laser weld in a cast Ti-6Al-4V alloy doped with 0.11 wt.% boron. It was found that prior β grain reconstruction could be performed successfully despite relatively low resolution and a large fraction of zero solutions in the as measured EBSD map. The β grain reconstruction and analysis of α variants highlighted differences in the transformed microstructures in each zone of the weld. The possibility to reconstruct β grains from low resolution α orientation maps will provide opportunity to optimize EBSD acquisition parameters enabling fast acquisition of large maps.

2. Experimental

A laser weld bead was produced on an 8.5 mm thick section of cast Ti-6Al-4V alloy doped with 0.11% boron. The chemical composition of the alloy is given in Table 1. After welding, cross section samples were cut out of the weld. Sample preparation was done using conventional metallographic techniques for titanium alloys, including grinding using SiC papers down to P2000. The final polish was carried out using OP-S polishing solution with H2O2. For optical microscopy, samples were etched with Kroll's etchant.

Table 1. Chemical composition (in wt.%) of cast Ti-6Al-4V-0.11B alloy

Al	V	B	O	Fe	C	N	H	Y	Ti
6.18	4.02	0.11	0.24	0.19	0.007	0.004	<0.001	<0.001	Bal

Scanning electron microscopy (SEM) and EBSD analyses were performed with a Zeiss Leo Gemini 1550 SEM equipped with Nordlys II detector and HKL Channel 5 software. A 4 µm step size was used to acquire overview orientation maps across the fusion zone (FZ), the heat affected zone (HAZ) and the base material. SEM and EBSD analyses were performed on unetched samples.

A numerical reconstruction of the parent β grains from the room temperature α phase EBSD data was performed using the *Merengue 2* software developed by Germain et al. [17], [18]. The method of reconstruction is based on the existence of the Burgers orientation relationship (BOR) between the body-centered cubic β phase and the hexagonal close packed α phase. The Burgers relation is satisfied whenever a $<2\bar{1}\bar{1}0>$ direction and a {0001} plane in the α phase coincide with a <111> direction and a {110} plane, respectively, in the β phase. As a result, a single β grain can transform into up to 12 α variants whose orientations can be deduced from the following relation [14]:

$$g\alpha_i = g\beta \times P_i \times \Delta g \qquad (1)$$

where $g\alpha_i$ represents the orientations of all variants, gβ the orientation of the parent β grain, P_i are the rotational symmetry elements of the parent phase and Δg is the BOR expressed as a rotation. Inversely, for an α variant, there exists six possible parent β grain orientations [19], [20]. The parent β grain orientation is then determined by selecting the orientation that is shared by most α variants and by excluding the variants that are not consistent with this parent orientation. In general, any combination of at least 4 α variants is always related to a unique potential parent β grain orientation [18]. There are also some combinations of two variants related to a unique parent. The best way to characterize those are the misorientations between variants. Wang et al. [20] showed that there exist 6 misorientation types between variants. They are listed in Table 2 with their probability of occurrence in absence of variant selection and with the number of potential parents related to both variants. This reveals that for two variants misoriented by either a type 3, 4 or 5 misorientation, a unique parent can be determined.

Table 2. Possible misorientation angles between *α* variants inherited from the same parent.

Type	Misorientation	P random	No. of potential parents
1	Identity	-	6
2	60° <1 1-2 0>	18.2 %	2
3	60.83° <-10-7 17 3>	36.4 %	1
4	63.26° <-10 5 5-3>	18.2 %	1
5	90° <7 -17 10 0>	18.2 %	1
6	10.53° <0001>	9.1 %	3

The as-measured EBSD orientation maps for the α phase can contain noise and a fraction of nonindexed pixels, so called zero solutions. Therefore, in most cases, the as-measured α orientation maps need to be corrected before applying the reconstruction method. The noise control can be performed using the commercial EBSD software. In a second step, the orientation of the neighboring pixels can be assigned to the zero solutions. Increasing the resolution of the α phase map, by reducing the step size of the measurement grid and using a higher magnification makes the indexing of small α variants possible which improves the reliability of determining the orientations of reconstructed β grains [18].

3. Results and discussion

3.1. Microstructure

In Fig. 1, the microstructure of a laser weld in cast Ti-6Al 4V-0.11B is shown. The weld was fully penetrated through the 8,5 mm section of the plate. The FZ is clearly visible and it is wider at the top and bottom with a narrower waist. The HAZ is also clearly distinguishable. Across the weld, the microstructure varied significantly. As shown in Fig. 1c, the base material had relatively coarse α colony type microstructure. The HAZ and the FZ have undergone a welding cycle and the rapid cooling had produced very fine Widmanstätten or colony type microstructure consisting of acicular α and α' as shown in Fig 1 b. As provided in Table 3, the α laths and α colonies were significantly finer in the HAZ and the FZ, respectively, than in the base material. Prior β grains in the base material and the HAZ were fairly equiaxed. In the base material and the HAZ, TiB particles were mainly located along the prior β grain boundaries. They revealed the shape of the prior β grains and made it possible to resolve prior β grains with optical microscopy. In the FZ, the absence of the grain boundary α layer and other α morphologies together with the significantly refined prior β grain size and TiB stripes inside the prior β grains made it impossible to resolve the prior β grains with optical microscopy. Only some of the high angle grain boundaries were visible at low magnification and ideal lighting conditions. Therefore, EBSD combined with β grains reconstruction was required for prior β grain characterization.

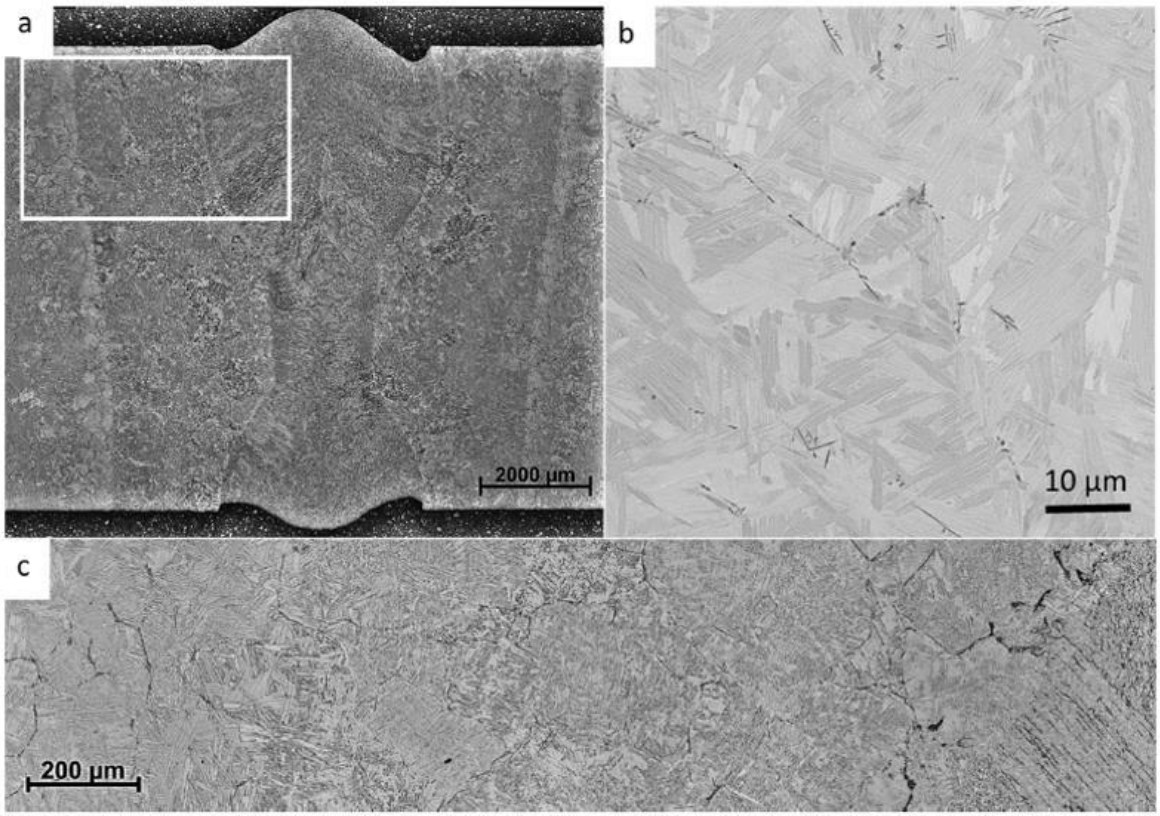

Figure 1. a) Optical micrograph of a laser weld in Ti-6Al-4V-0.11B showing the area of the EBSD map, b) SEM micrograph of the FZ showing the fine α colony microstructure and dark TiB particles, and c) optical micrograph showing the base material, the HAZ and the FZ (from left to right).

3.2. Reconstructed parent grains

A relatively large area of 3 x 5 mm was mapped to acquire the overview of the base material, the HAZ and the FZ of the laser weld. A step size of 4 µm was chosen to be able to acquire a map of such large area in a reasonable time. The as-measured orientation map of the α phase is shown in Fig. 2a in inverse pole figure coloring. Figure 2b shows the orientation map of the numerically reconstructed β phase. The step size was similar to the average size of the α colonies in the HAZ and the FZ. This means that data was not acquired from all the α colonies. The fine microstructure also resulted in a lower percentage of indexed points and lower quality of the EBSD patterns. The change in EBSD pattern quality is illustrated by the band contrast image in Fig. 2c. The zero solutions are shown in white in Fig. 2a. The fraction of the zero solutions and the size of microstructural features are given in Table 3. The indexing rate varied from 94% in the base material to 66% in the FZ. For improved indexing rate in these areas, a higher magnification would be needed since smaller step size does not improve indexing rate [21]. Other aspects affecting indexing rate may be sample preparation and the focus of the electron beam which can be inaccurate over such a large imaging area. The relatively low indexing rate did not seem to affect the quality of β grain reconstruction. Applying noise control and assigning the orientation of neighboring pixels to the zero solutions fills the map with the orientations of the measured α variants. This enables successful reconstruction even on a map with a relatively large fraction of zero solutions. Germain et al. [18] have been able to successfully reconstruct the β grains from an α phase orientation map with 60% indexing rate.

The reconstructed β grain map reveals the prior β grains in the different zones. In the base material and the HAZ, the prior β grains were relatively equiaxed and no significant grain growth was observed. The prior β grains in the FZ are narrow and elongated. In the FZ, the {100} β pole figure shows a weak texture typical for competitive growth during solidification where the <100> is close to the elongation direction of the grains. This texture was not seen in the base material. Figure 2b also shows that β grains nucleate and grow epitaxially from prior β grains in the HAZ but there are also large number of β grains nucleating within the FZ.

Table 3. Amount of zero solutions and size of microstructural features in different areas.

	Base material	Heat affected zone	Fusion zone
Zero solutions (%)	6.0	19.1	33.9
α lath thickness	3.9±1.3 µm	0.5±0.1 µm	0.5±0.1 µm
α colony size	23.4±3 µm	5.2±2.5 µm	4.7±1.2 µm
Prior β grain size	400-700 µm	400-700 µm	Columnar width 50-120 µm

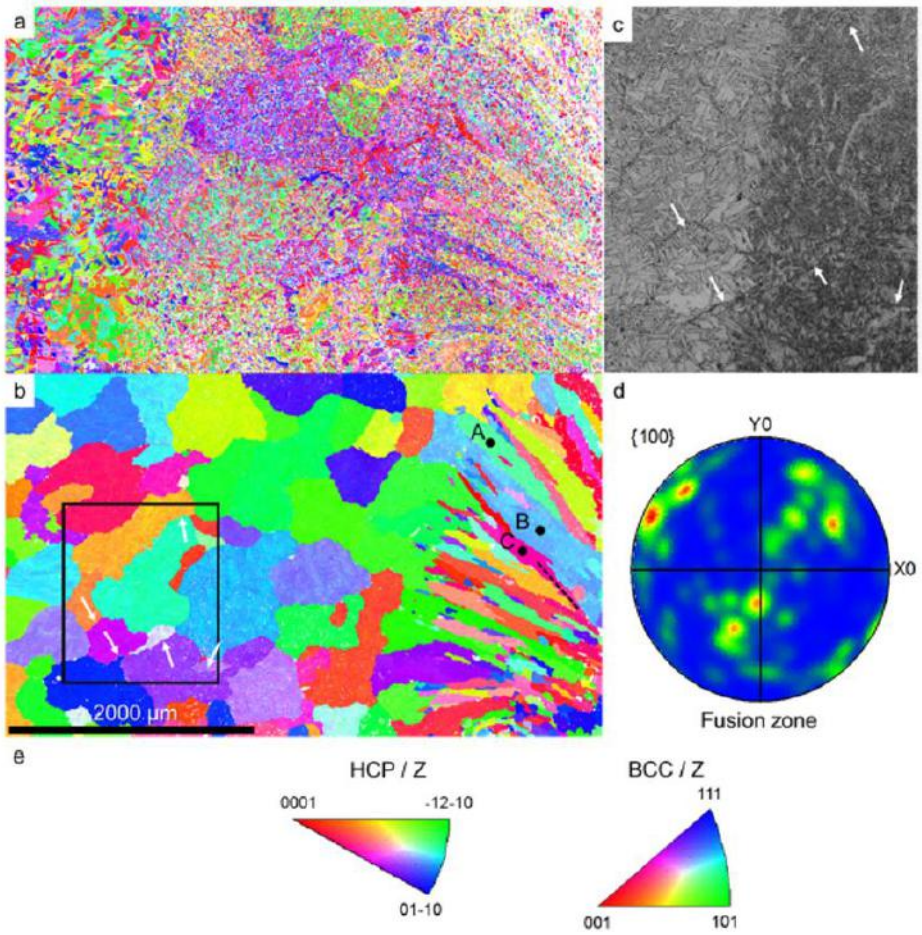

Figure 2. Prior β grain reconstruction of laser weld in Ti-6Al-4V-0.11B. a) as-measured inverse pole figure map of α phase, b) reconstructed β phase, c) magnified band contrast image, d) Pole figure of β phase in the FZ, and e) inverse pole figure color codes of hcp and bcc phase.

3.3. Transformation mechanisms studied from reconstructed grains

Base material, HAZ, and FZ show different microstructures due to the cooling rate and distribution of boron. The high cooling rate in the FZ promotes martensitic transformation while the cast base material has a relatively coarse α colony type microstructure as a result of low cooling rate and diffusional transformation [22]. If the orientation of the parent β grain was unique before transformation and if the BOR is strictly respected, every reconstructed grain should have a unique orientation according to equation (1). Any orientation deviation inside a parent grain indicates that one of the two condition is not strictly respected. Grain reference orientation deviation (GROD) maps can be used to quantify strain [23] but in case of reconstructed prior β maps in titanium alloys, they might be used to quantify the orientation deviations inside the grains.

As shown in Fig. 3, the different weld zones show distinct distributions of GROD (according to a color code). The FZ has on average the lowest GROD whereas in the HAZ the GROD is highest. In the as-cast material, the deviation is higher for some α colonies as well as in the vicinity of grain boundaries. This is typical for a diffusional phase transformation which follows the BOR with some noise. At a β grain boundary, the nucleation of α phase is influenced by the β grain next to it, and it is known to cause a slight deviation from the BOR to accommodate the transformation [24].This deviation can be seen also in the misorientation angle distribution (Fig. 4), as the type 4 and 6 variants in the as cast material have shifted whereas in the HAZ and FZ the misorientations between variants are closer to the theoretical angles.

The lower GROD in the FZ may be a result of higher cooling rate in the FZ resulting in martensitic transformation. Martensitic transformation is displacive and therefore the orientation relationship is more strictly respected. Indeed, diffusion occurs by moving vacancies which "shuffle" the position of the atoms, whereas in a strictly displacive mechanism, this does not occur. In the HAZ, cooling rate is lower which leads to a combination of diffusional and martensitic phase transformation and may explain the higher GROD.

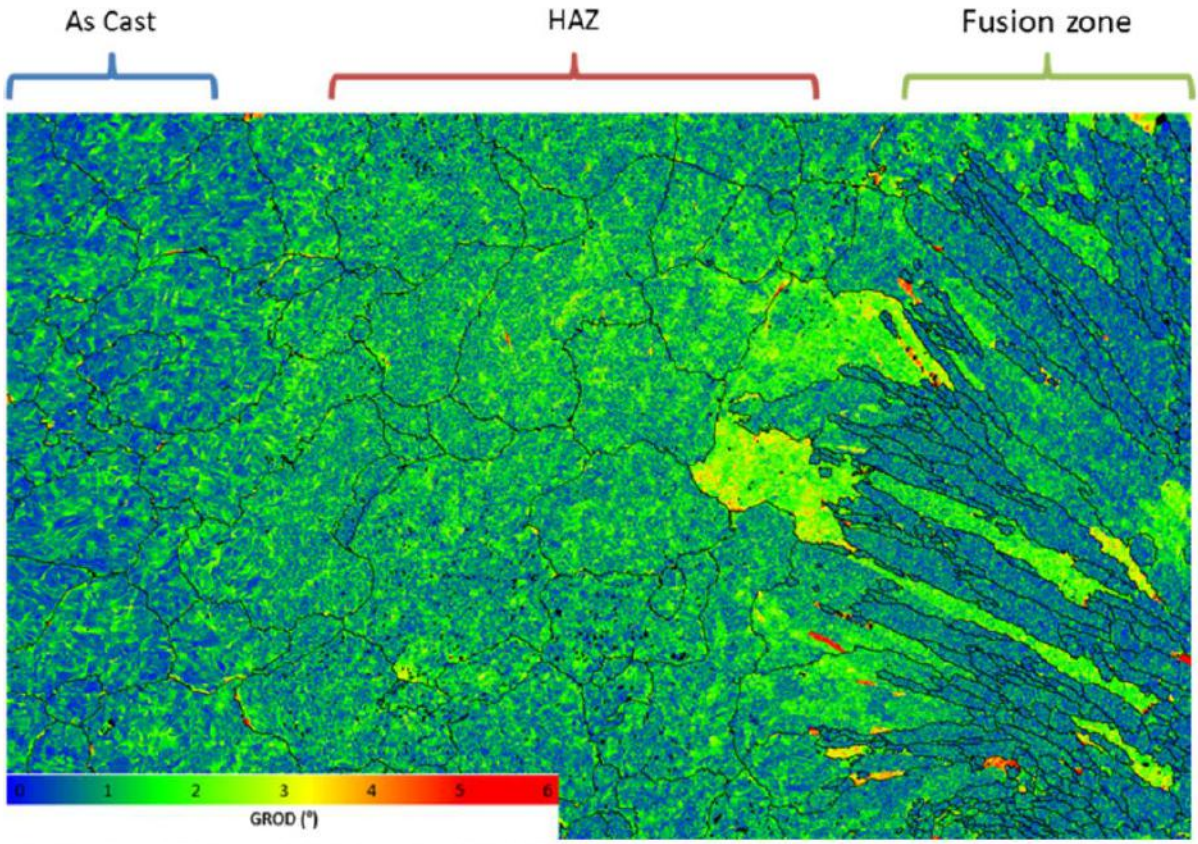

Figure 3. Grain reference orientation deviation map of a laser weld in Ti-6Al-4V-0.11B.

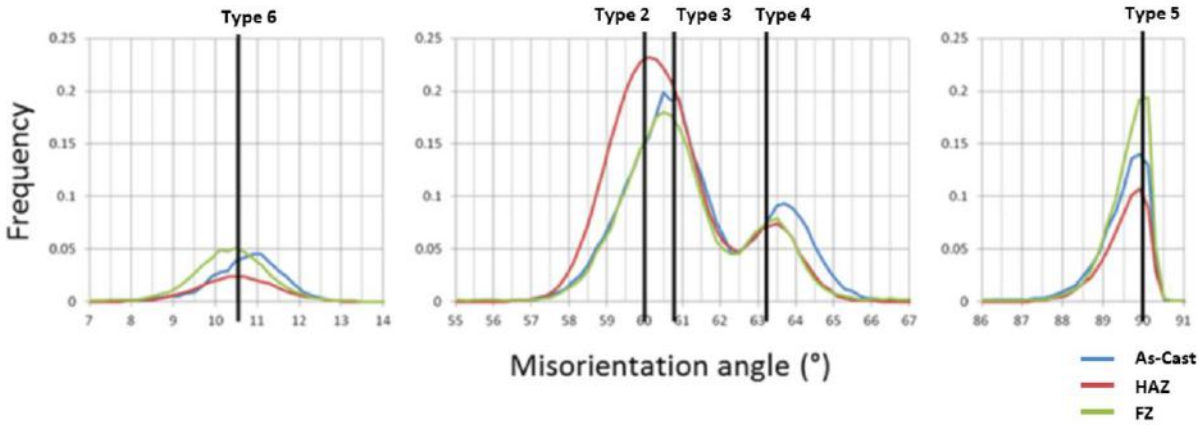

Figure 4. Misorientation angle distribution between α variants in the different weld zones.

Table 4. Inter-variant misorientation frequency in the different weld zones.

	As cast	HAZ	FZ	P random
type 2	35.4	63.9	38.4	18.2
type 3	25.4	14.7	20.3	36.4
type 4	25.0	14.6	20.2	18.2
type 5	6.4	4.0	11.7	18.2
type 6	7.8	2.8	9.4	9.1

There is also a difference in relative frequencies of α variant types as shown Fig. 4. For a proper interpretation, each misorientation type has to be compared to its theoretical frequency (P random) given in Table 2, and because of overlapping misorientation angles, it is important to consider misorientation axes as well. This was quantified in Table 4. As can be seen, the HAZ is dominated by type 2 variant. The FZ is also dominated by type 2, with also type 4 active. This is a result of auto-accommodation during martensite formation. Wang et al. [20] showed that two types of clusters of three variants minimize the shape strain during transformation. One cluster is characterized by three variants with type 2 misorientation and the other one by three variants with a type 4 misorientation. The results presented here show that both types of clusters are occurring but at a frequency which depends on the transformation conditions. These differences in variant selection and in GROD distribution indicate that the type of phase transformation was not the same in the three weld zones. However, further work is needed to quantify the effects from cooling rate and type of phase

transformation as well as the effect of TiB particles on nucleation of α phase at high cooling rates.

4. Summary

Prior β grain size and morphology of α phase affect the mechanical properties of welded and additively manufactured titanium alloys. Large grain size, columnar morphology and texture of prior β grains result in poor ductility and anisotropic behavior. Substantial effort has been put on decreasing the size of both β grains and α colonies. To evaluate the effect of these efforts, optimize the processing parameters and heat treatments as well as the chemistry of the alloys, robust and effective methods to characterize the size and orientation of β grains over relatively large regions are needed. In the present work, prior β grain reconstruction was performed successfully using Merengue 2 software on a laser weld in cast Ti-6Al-4V doped with boron. The prior β grain reconstruction revealed the prior β grain structure in the i) base material, ii) HAZ, and iii) FZ, and the reconstruction method proved to be robust. The original EBSD map was measured at low magnification and relatively large step size in comparison to the size of the α colonies. The fine microstructure together with low magnification resulted in a relatively low indexing rate in the FZ and HAZ, but this did not affect the quality of the prior β grain reconstruction. The possibility to reconstruct β grains from low resolution α orientation maps will provide opportunities to optimize EBSD acquisition parameters enabling fast acquisition of large maps. The analysis of α variants and the GROD map showing local deviations from the BOR that have occurred during β to α phase transformation, provide information about the nature of the phase transformation in the different weld zones.

5. Acknowledgements

The authors would like to acknowledge the financial support of NFFP (the Swedish National Program for Aeronautical Technology) and GKN Aerospace Engine Technologies for performing welding experiments. Dr. Lionel Germain for his help with the EBSD data analysis. Moreover, Mr. Maximilian Haack (University of Stuttgart) is also acknowledged for his help with optical microscopy.

6. References

1. K. K. Murthy, N. B. Potluri, and S. Sundaresan, *Material Science and Technology*, 13 (1997) 503-510.
2. T. Vilaro, C. Colin, and J. D. Bartout, Metallurgical and Materials Transactions A 42 (2011) 3190–3199.
3. G. Lütjering and J. C. William, Titanium. Springer-Verlag Berlin Heidelberg New York, 2003.
4. S. Sundaresan, G. D. Janaki Ram, and G. Madhusudhan Reddy, Materials Science & Engineering A, 262 (1999) 88-100.
6. R. Pederson, R. Gaddam, and M.-L. Antti, Central European Journal of Engineering, 2 (2012) 347-357.
7. S. Roy, S. Suwas, S. Tamirisakandala, D. B. Miracle, and R. Srinivasan, Acta Materialia, 59 (2011) 5494–5510.
8. S. Tamirisakandala, R. B. Bhat, D. B. Miracle, S. Boddapati, R. Bordia, R. Vanover, and V. K. Vasudevan, Scripta Materialia, 53 (2005) 217-222.
9. M. J. Bermingham, D. Kent, H. Zhan, D. H. StJohn, and M. S. Dargusch, Acta Materialia, 91 (2015) 289–303.
10. S. A. Mantri, T. Alam, D. Choudhuri, C. J. Yannetta, C. V. Mikler, P. C. Collins, and R. Banerjee, Journal of Materials Science, 52 (2017) 12455–12466.
11. Z. Mahbooba, H. West, O. Harrysson, A. Wojcieszynski, R. Dehoff, P. Nandwana, and T. Horn, JOM, 69 (2017) 472–478.
12. M. Simonelli, Y. Y. Tse, and C. Tuck, Journal of Materials Research, 29 (2014) 2028–2035.
13. M. G. Glavicic, P. A. Kobryn, T. R. Bieler, and S. L. Semiatin, Materials Science & Engineering A, 351 (2003) 258–264.
14. W. G. Burgers, Physica, 1 (1934) 561-586.
15. P. S. Davies, B. P. Wynne, W. M. Rainforth, M. J. Thomas, and P. L. Threadgill, Metallurgical and Materials Transactions A, 42 (2011) 2278-2289.
16. C. Cayron, Journal of Applied Crystallography, 40 (2007) 1183–1188.
17. L. Germain, N. Gey, R. Mercier, P. Blaineau, and M. Humbert, *Acta Materialia*, 60 (2012) 4551–4562.
18. L. Germain, N. Gey, and M. Humbert, *Ultramicroscopy*, 107 (2007) 1129–1135.
19. H. Beladi, Q. Chao, and G. S. Rohrer, *Acta Materialia*, 80 (2014) 478–489.
20. S. C. Wang, M. Aindow, and M. J. Starink, *Acta Materialia*, 51 (2003) 2485–2503.
21. Y. Chen, J. Hjelen, S. S. Gireesh, and H. J. Roven, *Journal of Microscopy*, 245 (2012) 111–118.
22. T. Ahmed and H. J. Rack, *Materials Science & Engineering A 243 (1998) 206-211*.
23. S. I. Wright, M. M. Nowell, and D. P. Field, *Microscopy and Microanalysis*, 17 (2011) 316–329.
24. N. Stanford and P. S. Bate, *Acta Materialia*, 52 (2004) 5215–5224.